Energy and Buildings

Development of new nano-enhanced phase change materials (NEPCM) to improve energy efficiency in buildings: lab-scale characterization

Marc Martín[1], Aida Villalba[1], A. Inés Fernández[1], Camila Barreneche[1,2,*]

[1]Department of Materials Science and Physical Chemistry, Universitat de Barcelona, Martí i Franqués 1–11, 08007 Barcelona, Spain

[2]Birmingham Centre for Energy Storage & School of Chemical Engineering, University of Birmingham, Birmingham B15 2TT, United Kingdom

*Corresponding author: c.barreneche@ub.edu

Abstract

Fatty acids are promising organic phase change materials (PCMs) for thermal energy storage (TES) in buildings because of their high storage capacity, non-toxic nature and little subcooling. Their phase change temperatures make them suitable for heating, ventilating and air conditioning (HVAC) applications in the building sector. However, one of their main drawbacks is their poor thermal conductivity which limits their application. In the present study two fatty acids within the building application temperature range, capric acid (CA) and capric - myristic acid (CA-MA) eutectic mixture, were nano-enhanced throughout silicon dioxide nanoparticles ($nSiO_2$) addition (0.5 wt.%, 1.0 wt.% and 1.5 wt.%). Main properties of the nano-enhanced phase change materials (NEPCM) obtained were characterized by means of differential scanning calorimetry (DSC), Hot wire technique, Fourier transformed infrared (FT-IR) spectroscopy, thermogravimetric analyses (TGA), scanning electron microscopy (SEM), and rheological measurements. Furthermore, their long-term performance was evaluated after 2000 cycles by means of cycling stability tests. The NEPCM obtained showed high thermal conductivity and specific heat capacity. Additionally, both are thermally stable within their working temperature range and ensure a long-term performance.

Keywords: Energy efficiency, Buildings, thermal energy storage (TES), latent heat, phase change material (PCM), nano-enhanced phase change materials (NEPCM), fatty acids, nanofluid, DSC, Hot wire.

1. Introduction

Developed countries still consume huge amount of energy whereas demand is rapidly increasing in developing countries. Nowadays, energy demand is mainly satisfied by non-renewable sources such as fossil fuels which have an effect on world climate. Building sector has attracted attention worldwide since the contribution from this sector towards global energy consumption. Taking into account residential and commercial applications, energy consumption has increased constantly, reaching more than 30% of total global final energy use in developed countries and has exceeded other sectors, such as transport and industry [1]. Moreover, the total building energy consumptions in BRIC countries (Brazil, Russia, India and China) have already exceed those in developed countries while its building stock is continuously increasing [2]. Thus, an improvement on building energy efficiency is mandatory. Heating, ventilating and air conditioning (HVAC) services represent 50% of building consumption and 20% of total consumption in the developed countries [1].

The use of proper thermal energy storage (TES) systems in building increase energy efficiency. In particular, phase change materials (PCMs) incorporation into buildings enables a more dynamic use of energy. One of the main gains of using PCMs in buildings lie in the peak load shifting of energy required for heating and cooling. Furthermore, due to latent heat thermal storage (LHTS) provided by PCMs thermal comfort is increased by temperature fluctuation reduction [3]. Other uses include, for example, achieving the peak-shifting strategy to improve the energy efficiency in domestic hot water applications [4]. These technologies are usually classified in active or passive systems. On one hand, passive TES systems take advantage of the daily temperature oscillation and/or seasonal temperature changes in buildings and reduce HVAC consumption. Passive strategies can be implemented into buildings in several manners, but so far the most common solution is by installing PCM enhanced wallboards towards the interior side of the building envelope. Thus, PCMs can improve thermal inertia of lightweigh structures, providing a significant increase in thermal storage capacity. Whereas, active TES systems are charged/discharged mechanically by the use of compressors, pumps or fans. These systems are able to be adapted to the energy production and demand using adequate control strategies [5].

According to ANSI/ASHRAE Standard 55-2013: *Thermal Environmental Conditions for Human Occupancy* the suggested room temperature for buildings is between 23.5 ºC - 25.5 ºC in the summer and between 21.0 ºC - 23.0 ºC during winter. The development of advanced materials to obtain high energy efficiency in buildings as phase change materials (PCM) which are able to store thermal energy is one of the key requirements in the building sector.

The proper selection of PCMs with suitable phase change temperature is crucial to obtain notable energy savings for total annual energy consumption. In generals terms, cooling dominant climates

require PCMs with melting temperatures close to 26 ºC whereas heating dominant climates require melting temperatures around 20 ºC in order to achieve higher annual energy savings [6]. Taking into account these scenarios, most fatty acids present a proper melting temperature range to be applied as PCMs in building applications – active systems: heating and cooling dominant climates. Moreover, fatty acids present great properties to be used as PCMs, such as high heat capacity, little or non-subcooling, congruent melting, low vapour pressure, non-toxic, thermal stability and non-corrosive to metal containers, low cost, small volume change and non-flammable [7]. Nevertheless, it is worth emphasizing that fatty acids present poor thermal conductivity, for instance in liquid state capric acid presents 0.150 W/m·K, stearic acid 0.172 W/m·K, lauric acid 0.147 W/m·K and palmitic acid 0.162 W/m·K [7]. These poor thermal conductivity values may slow down the heat exchange during storage and release processes.

Thus, many research studies have been carried out developing advance materials in order to enhance fatty acids thermal conductivity. Usually, these advanced materials consist on a PCMs doped with high surface to volume ratio materials such as nanomaterials, which enhance thermal conductivity and nucleation process. For instance, Palacios et al. [8] developed and analysed the thermal conductivity enhanced fatty acids with expanded graphite (EG) and powder graphite (PG). Zhang et al. [9] prepared palmitic-stearic acid (PA-SA) eutectic mixtures and enhanced by 20-30% its thermal conductivity with carbon nanotubes (CNTs) addition. For instance, fatty acids thermal conductivity also increases linearly with expanded graphite (EG) and carbon fibre (CF) addition. Karaipekli et at. [10] analysed the effect these materials in SA thermal properties, for 10 wt.% CF and EG content the thermal conductivity of the composite increased by 217.2% and 279.3%, respectively. Several authors enhanced PCMs thermal conductivity with nanoparticles addition, obtaining in that way nano-enhanced phase change materials NEPCM. A new type of NEPCM was developed by Wu et al. [11] with metallic nanoparticles. In this study, Al, Cu and C/Cu nanoparticles were added to melted paraffin and the obtained NEPCM characterized by means of differential scanning calorimetry (DSC) and Fourier transformed infrared (FT-IR) spectroscopy. Results obtained revealed the high cycling stability of this advanced material since the maximum change was -0.6% for melting temperature and 2% for freezing temperature after 100 melting-solidification cycles. Moreover, for NEPCM with 1.0 wt.% Cu nanoparticles the melting and solidification times were reduced by 30.3% and 28.2%, respectively. In another research study in 2014 Parameshwaran et al. [12] prepared a NEPCM based on fatty acid ester with silver-titania (Ag-TiO_2) nanoparticles addition ranging from 0.1 wt.% to 1.5 wt.%. This advanced material exhibited higher themal conductivity, from 0.286 W/m·K to 0.538 W/m·K, and a significant reduction in the subcooling (1.82 ºC). These values produce as a result a reduction in freezing and melting times, 23.9% and 8.5% respectively.

In the present paper, a new type of NEPCM was developed by adding SiO_2 nanoparticles to two fatty acids suitable for building applications. Furthermore, an exhaustive characterization was carried out in order to measure thermophysical properties, such as specific heat capacity (*Cp*), thermal conductivity (*k*), melting temperature (T_m) and enthalpy (ΔH_m). Furthermore, rheological behaviour was characterized and nanoparticle morphology observed throughout scanning electron microscopy (SEM).

2. Materials

2.1. Phase change materials (PCMs)

Two fatty acids have been selected to be used as phase change materials (PCMs) in order to be able to compare them and analyse how both behave while adding nanoparticles. Fatty acids belong to organic phase change materials and present some advantages over other type of PCMs such as chemical stability, melting congruency, low health hazard, high latent heat and phase change temperature within the building application range [13]. Taking into account that the PCMs with a phase change temperature between 18 ºC and 30 ºC are preferred in the building applications [14], capric acid (CA, $CH_3(CH_2)_8COOH$) and an eutectic mixture of myristic acid (MA, $CH_3(CH_2)_{12}COOH$) and CA have been selected. CA and MA were purchased from Sigma-Aldrich, both with ≥ 98% of purity.

CA/MA eutectic mixture ratio was 73.5 wt.% and 26.5 wt.% respectively. In order to produce the eutectic mixture both components were heated to a higher temperature to ensure liquid state. Meanwhile, fatty acids were stirred in a magnetic stirrer for 30 min at 400 rpm. Afterwards, eutectic mixtures were obtained by cooling down to room temperature.

Table 1 lists CA, MA and CA-MA eutectic mixture relevant properties found in the literature, i.e. melting enthalpy (ΔH_m), melting/solidification temperatures (T_m/T_s), specific heat capacity at constant pressure (C_p), and thermal conductivity (*k*).

Table 1. Phase change materials properties.

Materials	ΔH_m **(J/g)**	T_m/T_s **(ºC)**	C_p **(J/g·ºC)**	*k* **(W/m·K)**
Capric acid	152 [15]	31.82/26.54 [16]	2.77 [17]	0.153[7]
Myristic acid	199 [15]	54.55/49.28 [16]	1.90 [17]	0.150[7]
Eutectic mixture (73.5-26.5 wt.% CA-MA)	152 [15]	21.4/n.a [15]	n.a.	n.a.

n.a.- not available

2.2. Nano-enhanced phase change materials (NEPCM)

The two PCMs described in the prior sections were enhanced with silicon dioxide nanoparticles ($nSiO_2$) in four different concentrations obtaining eight different samples. Silicon dioxide nanoparticles were purchased from Sigma-Aldrich, present a 99.5% of purity, are spherical-porous shaped and present an average diameter of 5 nm to 15 nm. Using an analytical balance with 0.1 mg of precision, PCMs and nanoparticles were weighted in the right proportion. The preparation of nano-enhanced phase change materials (NEPCM) samples was performed using an ultrasonic probe (VCX 130 from Vibra-Cell) during 30 min obtaining around 40 g of each sample. In Table 2, composition of fatty acids samples is shown and the proportions of nanoparticles added to each one. The silicon dioxide nanoparticles cost is expected to be high and increase the cost of NEPCM, however, it has to be considered the quantities added, between 0.5 wt.% and 1.5 wt.%. In addition, the NEPCM will be more cost-effective as the production increases.

Table 2. Composition of enhanced fatty acids samples.

PCMs	SiO_2 nanoparticles proportion (wt.%)
Capric acid	0
	0.5
	1.0
	1.5
Eutectic mixture (73.5-26.5 wt.% CA-MA)	0
	0.5
	1.0
	1.5

3. Methodology

3.1. Thermophysical properties

Phase change materials have the capacity to store heat energy during melting and solidification processes (latent heat). Therefore, their key thermophysical properties that have been characterized are phase change temperature (T_m) and enthalpy (ΔH_m), while the storage of energy involves also sensible heat. Differential scanning calorimetry (DSC) is one of the most extensively used techniques to characterize TES materials thermophysical properties. Melting temperature, melting enthalpy and specific heat capacity at constant pressure measurements were

conducted in a Mettler Toledo DSC822e instrument under 50 mL/min N_2 flow. A first melting and solidification cycle was performed to ensure a suitable contact between sample and crucibles base. Samples were located in 40 µL aluminium crucibles. In melting enthalpy and melting temperature measurements temperature program used ranged temperature between 10 ºC and 50 ºC at 0.5ºC/min. Specific heat capacity under atmospheric pressure was measured at 40 ºC in liquid state throughout areas method proposed by Ferrer et al. [18] with a relative error below 3%.

3.2. Cycling stability

The cycling stability test was performed to study changes in chemical properties of the NEPCM after a large number of thermal cycles within the working temperature range of building applications.

Materials were cycled in a thermocycler (Bioer Gene Q T-18) and a tube of 0.5 mL was used to contain each sample. A dynamic method was established ranging temperature from 18 ºC to 40 ºC at 4 ºC/s for cooling and 5 ºC/s for heating. A total of 2000 cycles were performed under described conditions.

Chemical stability was analysed by means of Fourier transformed infrared (FT-IR) spectroscopy coupled with attenuated total reflectance (ATR). Samples IR spectrums were obtained and changes in characteristic peaks discussed. This analysis was carried out with a Spectrum Two™ from Perkin Elmer. The equipment standard spectral resolution is 0.5 cm^{-1} and was optimized within the 4000 – 350 cm^{-1} wavelength range. Thereby, aged samples were analysed after 2000 cycles with FT-IR and compared with no aged samples. Moreover, in order to analyse nanoparticles effect NEPCM spectra with 1.0 wt.% $nSiO_2$ were also obtained. Moreover, melting enthalpy and specific heat capacity of cycled NEPCM were measured following the same methodology described in previous section.

3.3. Thermal stability

Thermogravimetric analyses (TGA) were performed to study the NEPCM thermal degradation phenomenon obtaining wt.% as a function of temperature in this case. Initial degradation temperature is defined as the temperature achieved when the material loses 1.5 wt.% [19] compared to its initial weight. In addition, the final degradation temperature is defined as the temperature needed by the material to finish its thermal degradation process. Analyses were conducted in a simultaneous TGA/DSC DSTQ600 from TGA Instruments which has a balance

sensitivity of 0.1 µg. The heating rate used to perform the analysis was 10 ºC/min from 25 ºC to 500 ºC under 50 mL/min air flow. Opened 100 µL alumina crucibles used were filled with around 1/3 volume of material leading to average sample masses of around 15 mg.

3.4. Thermal conductivity

KD2 Pro Thermal properties analyser (Decagon Devices, Inc.) has been used for the measurement of thermal conductivity of NEPCM samples. The measurements were performed in liquid state at 45 ºC because significant improvements are expected in this state due to the effect of SiO_2 nanoparticles. Accordingly, the KS-1 Single Needle Sensor (6 cm) was used which has a ±0.01 W/m·K of accuracy from 0.02 W/m·K to 0.20 W/m·K and ±5% from 0.2 W/m·K to 2.0 W/m·K. This equipment use the transient hot-wire (THW) method used to measure nanofluids thermal conductivity [20].

3.5. Scanning electron microscopy (SEM)

A scanning electron microscope (SEM) from FEI, model Quanta 200 XTE 325/D8395, was used to determine the size of the incorporated nanoparticles. The electron beam used was 15 kV and the backscattered electron signal was depicted.

3.6. Rheological measurements

Since viscosity plays a key role in practical heat transfer scenarios and determines the pumping power required, a rheometer was used to characterize this property. The equipment used was a RST cone plate rheometer from AMETEK Brookfield which has a maximum torque of 100 mN·m with a resolution of 0.15 µN·m using Peltier air as control temperature device.
In addition, taking into account the measurement conditions established by Delgado et al.[21] and Zhang et al. [22], the rheometer experimental parameters were defined and are listed in Table 3.

Table 3. Rheometer experimental parameters.

Block	**Time (s)**	**Shear stress (Pa)**	**Shear rate (s^{-1})**	**Measurement points**
Rotation constant measuring block	20	Constant increment ratio	300	0
Rotation ramp measuring block	150	Constant increment ratio	350 to 5000	150

4. Results and discussion

4.1. Thermophysical properties

Specific heat capacity (*Cp*), melting enthalpy and melting temperature were measured by means of DSC technique. Thermal characterization is crucial in the present study since it measures the main properties for the PCMs purpose and where nanoparticle improvement takes place.

The DSC signal of the CA-MA mixture showed one sharp endothermic peak during the melting process, which indicates that the eutectic compound has been obtained, however it is not included in the present paper.

Table 4 shows CA and CA-MA melting temperature and melting enthalpy along with the PCMs enhanced via the addition of 0.5 wt.%, 1.0 wt.% or 1.5 wt.% $nSiO_2$ particles. At first sight CA and CA-MA eutectic mixture temperatures agreed with those reported in the literature [15] and [16]. However, melting temperature of both fatty acids slightly increased by nanoparticles addition. Enthalpy values around 150 J/g were also close to those reported in the literature. In general, after the addition of nanoparticles melting enthalpy of both fatty acids presented similar improvements, ranging from 6.8% to 10.7%. As it is observed, nano-enhanced CA-MA melting enthalpy was increased by a 6.8% regardless of the nanoparticles wt.%, whereas melting enthalpy of CA increases with nanoparticles content. However, enthalpy increments of nano-enhanced CA are detected for all formulations but the higher the nanoparticle content the lower the melting enthalpy increase for the same amount of nanoparticle addition.

Therefore, nano-enhanced CA-MA achieved 158 J/g and nano-enhanced CA up to 166 J/g with a 1.5 wt.% $nSiO_2$ content. Thus, the addition SiO_2 nanoparticles have a significant potential for enhancing the TES storage capacity of those fatty acids within the building application temperature range.

Table 4. Melting enthalpy (ΔH_m) and temperature (T_m) of nano-enhanced CA and CA-MA eutectic mixture.

Sample		**ΔH_m (J/g)**	**T_m (ºC)**
Capric acid		150	31.5
SiO_2 nanoparticles (wt.%)	**ΔH_m increment (%)**	**Nano-enhanced CA**	
0.5	8.0	162	31.2
1.0	10.0	165	31.2
1.5	10.7	166	31.2
Eutectic CA-MA mixture		148	21.9

SiO_2 nanoparticles (wt.%)	ΔH_m increment (%)	Nano-enhanced eutectic CA-MA	
0.5	6.8	158	22.0
1.0	6.8	158	22.1
1.5	6.8	158	22.1

A higher effect of the addition of $nSiO_2$ was obtained on the specific heat capacity; Table 5 shows the specific heat capacities measured for CA and CA-MA and its corresponding NEPCM. The results obtained show that the addition of nanoparticles to both fatty acids increases specific heat capacity around 20% in the liquid state (40 ºC). In particular, adding 1.0 wt.% of $nSiO_2$ produced the higher enhancement, in agreement with literature [23], [24], and [25]: a 23.5% in the CA-MA eutectic mixture and a 22.0% in the CA. Furthermore, the higher C_p, 3.38 J/g·ºC, was obtained with the addition of 1.0 wt.% of nanoparticles to CA. Consequently, nanoparticles added to these fatty acids allow the heat storage to be more effective per unit volume.

Table 5. Specific heat capacity (C_p) at 40 ºC of nano-enhanced CA and CA-MA.

Sample		C_p (J/g·ºC)
Capric acid		2.77
SiO_2 nanoparticles (wt.%)	***Cp* increment (%)**	**Nano-enhanced CA**
0.5	21.0	3.35
1.0	22.0	3.38
1.5	19.0	3.29
Eutectic CA-MA mixture		2.48
SiO_2 nanoparticles (wt.%)	***Cp* increment (%)**	**Nano-enhanced eutectic CA-MA**
0.5	20.4	2.99
1.0	23.5	3.07
1.5	20.4	3.00

As DSC analysis revealed, in general terms nanoparticles presence motivated high enhancements in *Cp* around 20%, while ΔH_m measured increment is between 6.8% and 10.7%. Thereby, a phase change process usually involves much more energy than a temperature change (ΔT=1ºC), and therefore melting enthalpy enhancement become diluted within the melting enthalpy values obtained. In addition, phase change enthalpy increments were not caused by the same mechanism as *Cp* since temperature remains constant during a phase change and *Cp* is by definition the energy required to increase one degree of temperature a specific mass under constant pressure [26].

4.2. Cycling stability

In order to characterize cycling stability NEPCM were analysed by means of FT-IR and DSC before and after 2000 cycles and results are shown in this section.

Cycling stability characterization by means of FT-IR allows to evaluate chemical degradation throughout IR spectra comparison: the appearance or disappearance of characteristic peaks indicate the formation of new bonds or the degradation of the existing, respectively [27]. Results obtained are shown in Figure 1, which revealed NEPCM stability after 2000 thermal cycles. Since CA and MA are saturated fatty acids with similar structure, CA and CA-MA eutectic mixture spectrums, Figure 1 a) and c), are very similar and many of its characteristic peaks coincide. Due to the alkane functionality of these fatty acids sharp peaks are observed in the 3000 cm^{-1} to 2850 cm^{-1} wavenumber range (sp^3 C-H stretching). The peak recorded at 1719 cm^{-1} correspond to the C=O stretching vibration, the 938 cm^{-1} peak correspond to the out of plane bending vibration and the 721 cm^{-1} peak correspond to the in-plane swinging vibration of functional group –OH [13]. Fatty acids, Figure 1 a) and c), do not degrade significantly due to thermal cycling since they showed equal characteristic peaks at 0 and 2000 cycles. Moreover, SiO_2 nanoparticles addition does not affect NEPCM cycling stability since equal spectrums were also obtained after thermal cycling for CA with 1.0 wt.% $nSiO_2$ (Figure 1 b), and CA-MA with 1.0 wt.% $nSiO_2$ (Figure 1 d). The rest of NEPCM samples with other nanoparticle proportion are expected to behave the same way not affecting fatty acids thermal cycling stability.

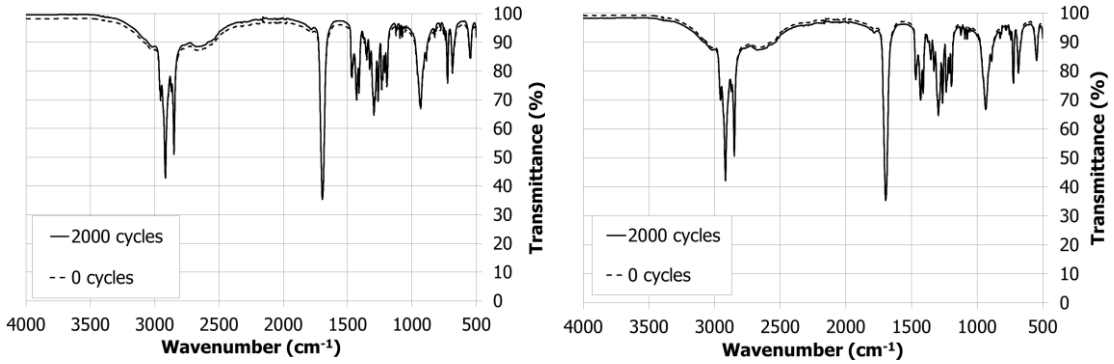

a) b)

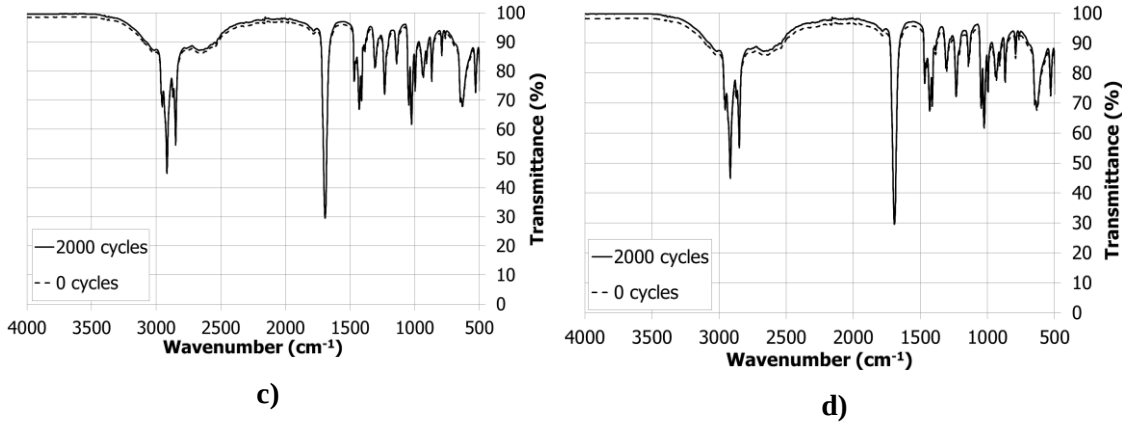

Figure 1. IR spectrums: a) CA b) CA with 1.0 wt.% $nSiO_2$ c) CA-MA d) CA-MA with 1.0 wt.% $nSiO_2$.

¡Error! La autoreferencia al marcador no es válida. shows the effect of thermal cycling on thermophysical properties (i.e. ΔH_m, T_m and C_p) along with percentile ΔH_m after 2000 cycles. As it can be seen thermal energy storage capacity and melting temperature were not significantly affected by thermal cycling including both fatty acids and NEPCM samples. The maximum ΔH_m variation due to thermal cycling was achieved in the CA-MA sample (+2.03%), however this value is within the measurement expected error (±10%) [28].

Table 6. Themal cycling results: ΔH_m, T_m and C_p before and after 2000 cycles.

Sample	Nº of cycles	ΔH_m (J/g)	C_p (J/g·ºC)	T_m (ºC)	ΔH_m after 2000 cycles (%)
CA	**0 cycles**	150	2.77	31.5	+0.67
	2000 cycles	151	2.81	31.5	
CA with 1.0 wt.% $nSiO_2$	**0 cycles**	165	3.38	31.2	+0.61
	2000 cycles	166	3.33	31.2	
CA-MA	**0 cycles**	148	2.48	21.9	+2.03
	2000 cycles	151	2.51	22.0	
CA-MA with 1.0 wt.% $nSiO_2$	**0 cycles**	158	3.07	22.1	-0.63
	2000 cycles	157	3.11	22.0	

4.3. Thermal stability

When designing a thermal energy storage (TES) system, it is of crucial importance to ensure thermal stability of the materials used [19]. Thermogravimetric analyses (TGA) have been performed to study the thermal decomposition of the materials and ensure that initial degradation temperature is higher than the working temperature range of building applications.

First, the thermal stability of CA and CA-MA are plotted in Figure 2. It is observed that the degradation of these materials consists on one-step that starts at 120 ºC and ends between 210 ºC and 240 ºC. As it can be seen, the decomposition of both materials starts at 120 ºC and therefore authors confirm that the PCMs and the NEPCM under development are stable within the buildings applications temperature range. Notice that thermal degradation process of NEPCM finishes at similar temperatures, which is expected since their matrix is the same. As it is shown in TGA curves, SiO_2 nanoparticles do not affect thermal degradation process of the analysed nano-enhanced CA while slight improvements are observed in nano-enhanced CA-MA.

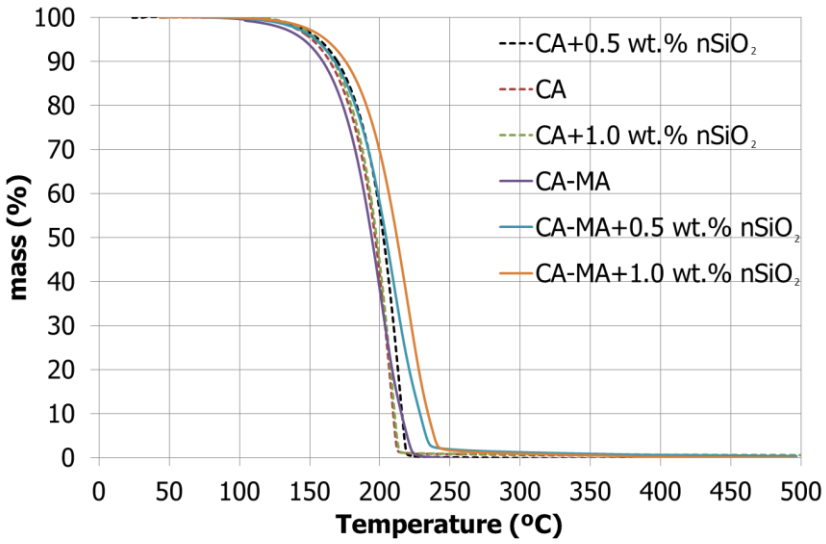

Figure 2. NEPCM thermogram: wt.% mass as function of temperature.

4.4. Thermal conductivity

The thermal conductivity (*k*) has been measured in liquid state at 45 ºC. Thermal conductivity as function of nanoparticles content in both fatty acids is depicted in Figure 3. The thermal conductivity of the NEPCM increases as the amount of $nSiO_2$ increases. Taking into account the results obtained, CA presented the highest thermal conductivity before (0.296 W/m·K) and after the addition of nanoparticles (0.529 W/m·K) for the NEPCM with 1.5 wt.%.

However, CA-MA presented an outstanding thermal conductivity increase, up to 142% for the 1.5 wt.% $nSiO_2$ sample, due to nanoparticles addition. As results revealed, the higher the nanoparticles content, the higher the thermal conductivity. This could be explained taking into consideration some phenomena such as: Brownian motion, phonon interaction, clustering of nanoparticles and surface morphology effects [29] and [30].

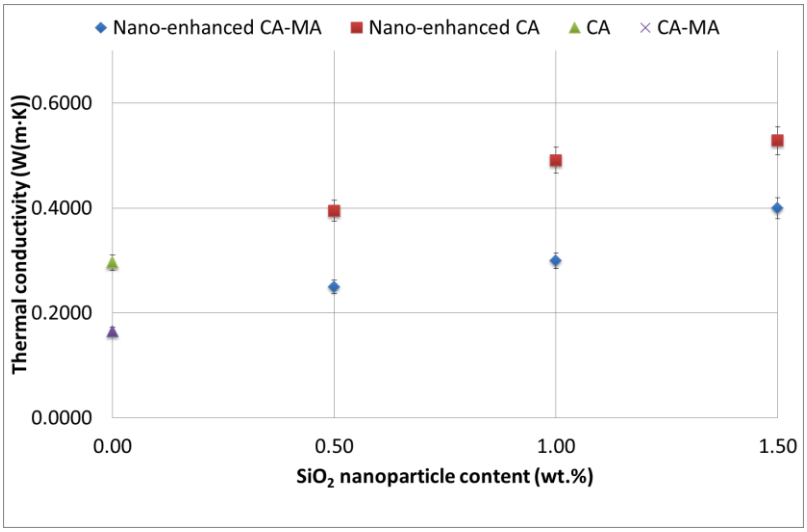

Figure 3. Thermal conductivity (W/m·K) as function of SiO_2 nanoparticle content (wt.%).

In spite of many desirable properties of fatty acids, the disadvantage of low thermal conductivity reduce their potential application in buildings since limits its heat transfer capacity. The addition of nanoparticles to fatty acids improved one of the main drawbacks of this type of PCMs by enhancing its heat transfer between the system and the media. Therefore, the fatty acids main drawback is turned into one the main nano-enhanced fatty acids strengths. Thereby, the fatty acids group pass from the bottom part of the chart where is represented the thermal conductivity vs. latent heat of fusion to the upper part as Figure 4 shows.

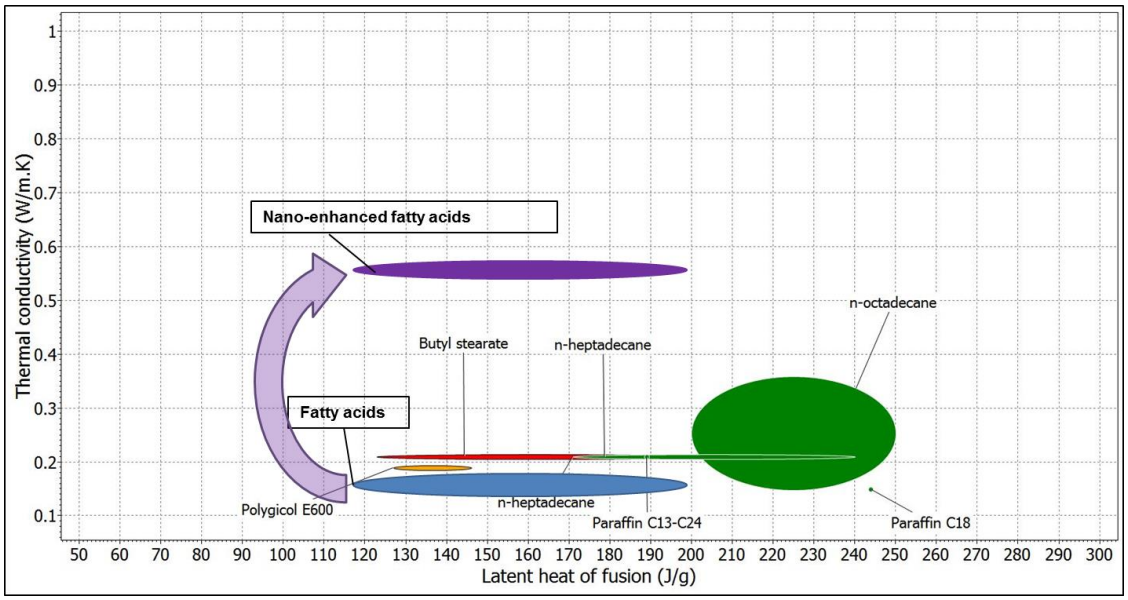

Figure 4. Chart of organic PCMs that plots latent heat of fusion (ΔH_m) vs. thermal conductivity (k), adapted from [31].

4.5. Scanning electron microscopy (SEM)

Silicon dioxide nanoparticles were commercial and are spherical-porous shaped. Nanoparticles present an average diameter of 5 nm to 15 nm according to manufacturer. Results from the scanning electron microscopy (SEM) are shown in Figure 5 with two magnifications: x35000 and x65000, respectively. As it is demonstrated $nSiO_2$ aggregate forming clusters of 100 nm to 300nm. Experimental evidences [29] strongly suggest that clustering phenomena promotes the thermal conductivity enhancements demonstrated in this study.

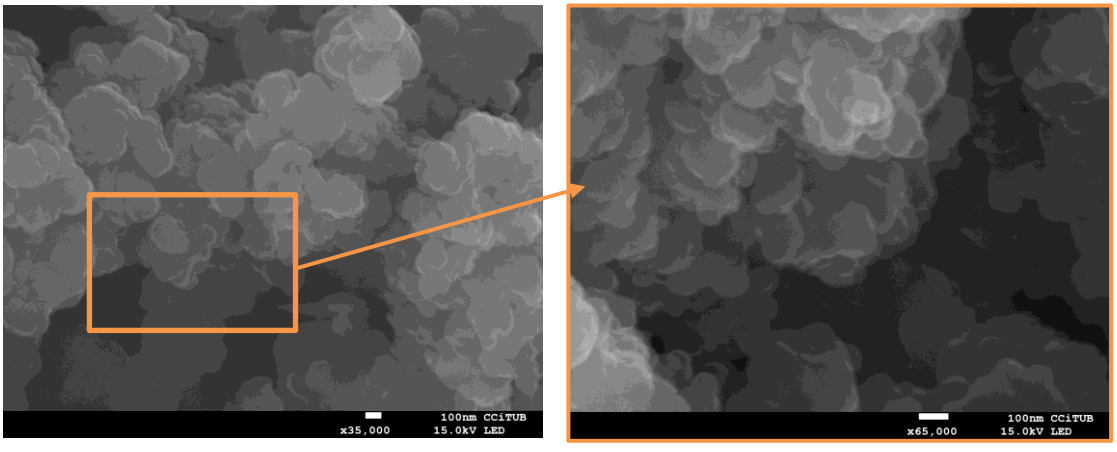

a) b)

Figure 5. The SEM images of $nSiO_2$. Magnification: a) x 35000 b) x65000.

4.6. Rheological behaviour

Rheological characterization is since it determines how the fluid behaves and how $nSiO_2$ particles affect it. NEPCM in liquid state constitutes a nanofluid since it is defined as fluid containing nm-sized particles. It is well known that viscosity of nanofluids is greatly dependent on particle aggregation phenomena, temperature and nanoparticles content, size and shape [32].

As it can be seen both NEPCM showed Newtonian behaviour since viscosity *(η)* do not depend on shear rate (Figure 6). Moreover, NEPCM viscosity increases linearly as the amount of nanoparticle increases especially in CA. Usually, the relationship between viscosity and temperature strongly depends on particle size and concentration. However, building applications present low temperature gradients and temperature effect could be negligible.

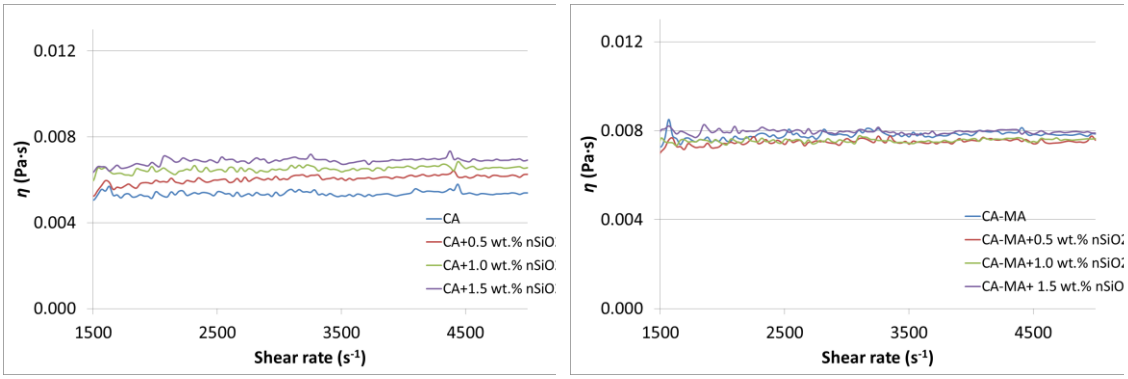

a) b)

Figure 6. *η* as function of shear rate of NEPCM: a) based on CA b) based on CA-MA.

5. Conclusions

Both fatty acids, CA and CA-MA eutectic mixture, were enhanced with SiO_2 nanoparticles addition up to 1.5 wt.%. Thermal conductivity and specific heat capacity of both PCMs were significantly enhanced by nanoparticles.

Experimental results showed outstanding increments in NEPCM thermal conductivity, for instance CA-MA thermal conductivity was increased up to 142% with the addition of 1.5 wt.% $nSiO_2$. The results clearly showed an almost linear relationship between thermal conductivity and $nSiO_2$ content. Sensible heat storage capacity was significantly improved since specific heat capacity measurements showed an increment of around 20% in both fatty acids, besides the higher improvements were obtained with 1.0 wt.% nanoparticle content. Whereas, latent heat storage capacity improvements were lower, in any case, noteworthy melting enthalpies were measured: 158 J/g for CA-MA+1.5 wt.% $nSiO_2$ and 166 J/g for CA+1.5 wt.% $nSiO_2$. Furthermore, TGA showed that both fatty acids are stable within the building working temperature range. Moreover,

nanoparticle content does not affect CA thermal stability while slightly improves CA-MA thermal stability. Cycling stability tests demonstrated that thermophysical (i.e. ΔH_m, T_m and C_p) and chemical properties of both NEPCM remain almost constant after 2000 thermal cycles. Finally, both NEPCM were characterized as a nanofluid throughout rheological measurements. Results revealed its Newtonian behaviour and how viscosity nearly increases linearly with nanoparticles mass fraction.

To summarize, two fatty acids with melting points within the building application range, CA (31.5 ºC) and CA-MA (21.9 ºC), were successfully enhanced via SiO_2 nanoparticles addition. The NEPCM obtained showed high thermal conductivity and specific heat capacity. In addition both are thermally stable within their working temperature range and ensure a long-term performance. As fatty acids have a poor thermal conductivity for the PCM purpose, it should be the key direction of development to combine them and form composite PCMs as the NEPCM developed in the present study. However, cost is another barrier to the use of NEPCM so future research should work on doing this composite materials more cost-effective, which would allow its application in real environments. One key point that has to be developed is nanomaterials production methods scalability. Despite the fact that several production methods are available at laboratory-scale, only a minority of them is used for large-scale production nowadays. Likewise, each production method has a limited range of materials that can be produced in a viable manner.

Acknowledgements

The work was partially funded by the Spanish government (ENE2015-64117-C5-2-R (MINECO/FEDER)). The authors would like to thank the Catalan Government for the quality accreditation given to its research group DIOPMA (2017 SGR 118). DIOPMA is certified agent TECNIO in the category of technology developers from the Government of Catalonia. The research leading to these results has received funding from the European Union's Horizon 2020 research and innovation programme under the Marie Skłodowska-Curie grant agreement No 712949 (TECNIOspring PLUS) and from the Agency for Business Competitiveness of the Government of Catalonia.

References

[1] L. Pérez-Lombard, J. Ortiz, and C. Pout, "A review on buildings energy consumption information," *Energy Build.*, vol. 40, no. 3, pp. 394–398, Jan. 2008.

[2] U. Berardi, "A cross-country comparison of the building energy consumptions and their trends," *Resour. Conserv. Recycl.*, vol. 123, pp. 230–241, 2017.

[3] S. E. Kalnæs and B. P. Jelle, "Phase change materials and products for building applications: A state-of-the-art review and future research opportunities," *Energy Build.*, vol. 94, no. 7491, pp. 150–176, 2015.

[4] M. Mazman, L. F. Cabeza, H. Mehling, M. Nogues, H. Evliya, and H. O. Paksoy, "Utilization of phase change materials in solar domestic hot water systems," *Renew. Energy*, vol. 34, no. 6, pp. 1639–1643, 2009.

[5] A. de Gracia and L. F. Cabeza, "Phase change materials and thermal energy storage for buildings," *Energy Build.*, vol. 103, pp. 414–419, 2015.

[6] M. Saffari, A. de Gracia, C. Fernández, and L. F. Cabeza, "Simulation-based optimization of PCM melting temperature to improve the energy performance in buildings," *Appl. Energy*, vol. 202, pp. 420–434, 2017.
[7] Y. Yuan, N. Zhang, W. Tao, X. Cao, and Y. He, "Fatty acids as phase change materials: A review," *Renew. Sustain. Energy Rev.*, vol. 29, no. January, pp. 482–498, 2014.
[8] A. Palacios, A. de Gracia, L. F. Cabeza, E. Julià, A. I. Fernández, and C. Barreneche, "New formulation and characterization of enhanced bulk-organic phase change materials," *Energy Build.*, vol. 167, pp. 38–48, 2018.
[9] N. Zhang, Y. Yuan, Y. Yuan, X. Cao, and X. Yang, "Effect of carbon nanotubes on the thermal behavior of palmitic-stearic acid eutectic mixtures as phase change materials for energy storage," *Sol. Energy*, vol. 110, no. October 2017, pp. 64–70, 2014.
[10] A. Karaipekli, A. Sari, and K. Kaygusuz, "Thermal conductivity improvement of stearic acid using expanded graphite and carbon fiber for energy storage applications," *Renew. Energy*, vol. 32, no. 13, pp. 2201–2210, 2007.
[11] S. Wu, D. Zhu, X. Zhang, and J. Huang, "Preparation and melting/freezing characteristics of Cu/paraffin nanofluid as phase-change material (PCM)," *Energy and Fuels*, vol. 24, no. 3, pp. 1894–1898, 2010.
[12] R. Parameshwaran, K. Deepak, R. Saravanan, and S. Kalaiselvam, "Preparation, thermal and rheological properties of hybrid nanocomposite phase change material for thermal energy storage," *Appl. Energy*, vol. 115, pp. 320–330, 2014.
[13] A. Karaipekli and A. Sari, "Capric-myristic acid/vermiculite composite as form-stable phase change material for thermal energy storage," *Sol. Energy*, vol. 83, no. 3, pp. 323–332, 2009.
[14] D. Zhou, C. Y. Zhao, and Y. Tian, "Review on thermal energy storage with phase change materials (PCMs) in building applications," *Appl. Energy*, vol. 92, pp. 593–605, 2012.
[15] A. Sharma, V. V. Tyagi, C. R. Chen, and D. Buddhi, "Review on thermal energy storage with phase change materials and applications," *Renew. Sustain. Energy Rev.*, vol. 13, no. 2, pp. 318–345, 2009.
[16] Z. Zhang, Y. Yuan, N. Zhang, and X. Cao, "Thermophysical Properties of Some Fatty Acids/Surfactants as Phase Change Slurries for Thermal Energy Storage," *J. Chem. Eng. Data*, vol. 60, no. 8, pp. 2495–2501, 2015.
[17] C. . Schaake, R.C.F.; van Miltenburg, J.C.; De Kruif, "Thermodynamic properties of the normal alkanoic acids. II. Molar heat capacities of seven even-numbered normal alkanoic acids," *Chem. Thermodyn.*, no. 14, pp. 771–778, 1982.
[18] G. Ferrer, C. Barreneche, A. Solé, I. Martorell, and L. F. Cabeza, "New proposed methodology for specific heat capacity determination of materials for thermal energy storage (TES) by DSC," *J. Energy Storage*, vol. 11, pp. 1–6, 2017.
[19] J. Gasia, M. Martin, A. Solé, C. Barreneche, and L. F. Cabeza, "Phase change material selection for thermal processes working under partial load operating conditions in the temperature range between 120 and 200 °C," *Appl. Sci.*, vol. 7, no. 7, 2017.
[20] G. Paul, M. Chopkar, I. Manna, and P. K. Das, "Techniques for measuring the thermal conductivity of nanofluids: A review," *Renew. Sustain. Energy Rev.*, vol. 14, no. 7, pp. 1913–1924, 2010.
[21] M. Delgado, A. Lázaro, C. Peñalosa, and B. Zalba, "Experimental analysis of the influence of microcapsule mass fraction on the thermal and rheological behavior of a PCM slurry," *Appl. Therm. Eng.*, vol. 63, no. 1, pp. 11–22, 2014.
[22] G. H. Zhang and C. Y. Zhao, "Synthesis and characterization of a narrow size distribution nano phase change material emulsion for thermal energy storage," *Sol. Energy*, vol. 147, pp. 406–413, May 2017.
[23] R. Hentschke, "On the specific heat capacity enhancement in nanofluids," *Nanoscale Res. Lett.*, vol. 11, p. 88, Feb. 2016.
[24] M.-C. Lu and C.-H. Huang, "Specific heat capacity of molten salt-based alumina

nanofluid," *Nanoscale Res. Lett.*, vol. 8, no. 1, p. 292, Jun. 2013.
[25] H. Zhu, C. Zhang, S. Liu, Y. Tang, and Y. Yin, "Effects of nanoparticle clustering and alignment on thermal conductivities of Fe_3O_4 aqueous nanofluids," *Appl Phys Lett*, vol. 89, 2006.
[26] D. Halliday, J. Walker, and R. Resnick, *Fundamentals of Physics*. Wiley, 2013.
[27] E. Pretsch, *Determinación estructural de compuestos orgánicos*. Elsevier España, S.L., 2002.
[28] H. Mehling, H. P. Ebert, and P. Schossig, "Development of standards for materials testing and quality control of PCM," *7th IIR Conf. Phase Chang. Mater. Slurries Refrig. Air Cond. Fr.*, no. c, pp. 1–9, 2006.
[29] J. W. Gao, R. T. Zheng, H. Ohtani, D. S. Zhu, and G. Chen, "Experimental investigation of heat conduction mechanisms in nanofluids. Clue on clustering," *Nano Lett.*, vol. 9, no. 12, pp. 4128–4132, 2009.
[30] D. Kim *et al.*, "Convective heat transfer characteristics of nanofluids under laminar and turbulent flow conditions," *Curr. Appl. Phys.*, vol. 9, no. 2 SUPPL., 2009.
[31] C. Barreneche, H. Navarro, S. Serrano, L. F. Cabeza, and A. I. Fernández, "New Database on Phase Change Materials for Thermal Energy Storage in Buildings to Help PCM Selection," *Energy Procedia*, vol. 57, pp. 2408–2415, 2014.
[32] B. S. Zan Wu, Zhaozan Feng, Lars Wadso, "Thermal Conductivity and Rheology Behavior of Aqueous Nanofluids Containing Alumina and Carbon Nanotubes," *4th Micro Nano Flows Conf.*, no. September, pp. 7–10, 2014.